

# Lab on a Chip

Accepted Manuscript



This is an *Accepted Manuscript*, which has been through the Royal Society of Chemistry peer review process and has been accepted for publication.

*Accepted Manuscripts* are published online shortly after acceptance, before technical editing, formatting and proof reading. Using this free service, authors can make their results available to the community, in citable form, before we publish the edited article. We will replace this *Accepted Manuscript* with the edited and formatted *Advance Article* as soon as it is available.

You can find more information about *Accepted Manuscripts* in the [Information for Authors](#).

Please note that technical editing may introduce minor changes to the text and/or graphics, which may alter content. The journal's standard [Terms & Conditions](#) and the [Ethical guidelines](#) still apply. In no event shall the Royal Society of Chemistry be held responsible for any errors or omissions in this *Accepted Manuscript* or any consequences arising from the use of any information it contains.

Cite this: DOI: 10.1039/c0xx00000x

www.rsc.org/xxxxxx

ARTICLETYPE

# Microfluidic studies of polymer adsorption in flow

Zhaoyi Wang,<sup>a,b</sup> Dan Voicu,<sup>a</sup> Ling Tang,<sup>c,d</sup> Wei Li,<sup>d\*</sup> and Eugenia Kumacheva,<sup>a\*</sup>

Received (in XXX, XXX) Xth XXXXXXXXX 20XX, Accepted Xth XXXXXXXXX 20XX

DOI: 10.1039/b000000x

## Abstract

Adsorption of polymers from solutions moving past solid or liquid surfaces controls a broad range of phenomena in science, technology, and medicine. In the present work, a microfluidic methodology was developed to study polymer adsorption in flow under well-defined conditions by integrating an attenuated total reflection-Fourier transform infrared (ATR-FTIR) spectroscopy with a microfluidic device. Polymer adsorption in flow was studied for exemplary polyelectrolytes such as polystyrene sulfonate and polyacrylic acid under varying flow rates, polymer concentrations, pH, and ionic strengths of the solution. Furthermore, the microfluidic platform was utilized to study layer-by-layer adsorption of alternating anionic and cationic polyelectrolytes such as polyacrylic acid and polyallylamine hydrochloride. The proposed methodology paves the way for studies of in-flow adsorption of biologically relevant molecules, which would mimic processes occurring in the cardiovascular microcirculation system.

## Introduction

Adsorption of polymers on liquid and solid surfaces has a vast range of applications in science and technology, including the stabilization of colloid particles, adhesion, lubrication, control of wetting phenomena, compatibilization of otherwise incompatible phases, and site-specific drug delivery.<sup>1-3</sup> Polymer molecules and their supramolecular assemblies undergo adsorption from their quiescent solutions, when an attraction energy between the polymer and the surface exceeds the entropy loss upon adsorption.<sup>4</sup> In the absence of flow, polymer adsorption includes three successive steps, namely, diffusion of macromolecules to a surface, attachment to the surface, and chain relaxation toward its equilibrium state.<sup>4</sup>

Less attention has been paid to adsorption of polymers from solutions moving past solid or liquid surfaces, although this phenomenon is important for a broad range of disciplines, including tribology, biology, and medicine.<sup>5</sup> For example, the formation of biofilms is initiated by adsorption of macromolecules from the aqueous milieu to the surface of rocks, sewage pipes, teeth, or boat hulls.<sup>6,7</sup> The formation and growth of thrombi occurs under the flow of blood, which imparts shear forces on adsorbing fibrin(ogen) and transports coagulation factors and anticoagulation molecules to and from the thrombus and blood vessel walls.<sup>8</sup>

Polymer adsorption in flow exhibits at least, three additional features, in comparison with adsorption under quiescent conditions, that is, the change in molecular conformation and orientation due to hydrodynamic forces, the competition between polymer adsorption and its transverse motion past the surface, and the shear force affecting the orientation and conformation of polymer molecules on the surface.

Polymer adsorption is generally studied by ellipsometry,<sup>9-11</sup> atomic force microscopy (AFM),<sup>12</sup> total internal reflection fluorescence,<sup>13-15</sup> radiolabeling,<sup>16</sup> quartz crystal microbalance,<sup>17</sup> and attenuated total reflection-Fourier transform infrared (ATR-

FTIR) spectroscopy<sup>18,19</sup> techniques. Among these methods, ATR-FTIR spectroscopy is a label-free, non-destructive tool with the capability to detect multiple components simultaneously in a fast, cost- and labor-efficient manner,<sup>20,21</sup> which can be used to study polymer adsorption under static and dynamic conditions. Moreover, ATR-FTIR spectroscopy can provide detailed molecular-level information on the conformation or orientation of macromolecules on the surface.<sup>22</sup>

Integration of ATR-FTIR with microfluidic (MF) devices offers the ability to study adsorption of polymers in flow under highly controllable shear rates, in addition to the benefits of low reagent consumption, the capability of high-throughput change in the composition of polymer solutions, and excellent control over heat and mass transfer.<sup>23-26</sup> The MF-integrated ATR-FTIR characterization tool has been utilized to study the composition of multicomponent polymer solutions,<sup>27</sup> and kinetics of polymerization reactions.<sup>28</sup> In addition, the FTIR imaging platform was utilized to obtain chemical information on reactants and products at different points of time and at different locations of the MF device.<sup>29-31</sup> Yet, since ATR-FTIR spectroscopy acquires information on the analyte present both on the surface of the ATR crystal and up to several micrometers from the crystal surface, the characterization of polymer adsorbed on the surface, rather than in the polymer solution in the vicinity of the surface is yet to be studied.

In the present work, we used ATR-FTIR spectroscopy integrated with a MF device to explore adsorption of single-component polyelectrolyte layers under different flow rate conditions from solutions with varying polymer concentration, pH, and ionic strength. The ATR-FTIR technique integrated with microfluidics characterizes changes in the IR spectra of analytes both in the solution flowing past the ATR crystal (typically, several micrometers away from the crystal surface) and in the analyte adsorbed on the crystal surface. In our earlier work, we characterized polymers in the solution flowing past the ATR

crystal<sup>32</sup> and studied polymerization kinetics in solution<sup>28</sup>. In the present work, we focused only on the polymer adsorbed on the ATR-crystal surface.

To show the versatility of the method, we applied it to study in-flow adsorption of multi-component, layer-by-layer (LbL) polymer layers of alternating anionic and cationic polyelectrolyte layers.<sup>33-36</sup> For the L-b-L adsorption, we selected polyacrylic acid and polyallylamine hydrochloride as complementary polymers due to (i) their propensity to form stable complexes in aqueous solutions<sup>37,38</sup> and (ii) the presence carboxylic acid and amine functional groups,<sup>70</sup> which are common for biological<sup>39</sup> and synthetic<sup>40</sup> and can be readily identified using IR spectroscopy.<sup>41</sup> The developed methodology combines the advantages of ATR-FTIR characterization and MFs. It paves the way for studies of in-flow adsorption of biologically relevant molecules, which would mimic processes occurring in the cardiovascular microcirculation system.

## Materials and methods

Polystyrene sulfonate, polyacrylic acid, polyallylamine hydrochloride with the average molecular weights of 70 000, 450 000, and 58 000 g mol<sup>-1</sup>, respectively, were purchased from Sigma-Aldrich Canada and used as received. Tris(hydroxymethyl)aminomethane (99+%) (Tris) and piperidine (99.5+%) were purchased from Sigma-Aldrich Canada. Phosphoric acid was purchased from Caledon Laboratories Ltd. Sodium chloride was purchased from ACP Chemicals (Quebec, CA). Photoresist (SU-8 3050) and SU-8 developer were supplied by Microchem Corporation (USA). Polycarbonate (PC) (Lexan 9034-112) was supplied by Sabic (USA) and dehydrated by pre-heating at 80 °C for 40-80 min before embossing. Polycarbonate film with a thickness of 175 µm was purchased from McMaster Carr (USA). Deionized water was purified using a Milli-Q Plus purification system (Millipore Corp., USA). Viscosity of the polymer solution was measured with a programmable rheometer (Brookfield, Model DV-III) at room temperature.

The MF device was fabricated using a thermoembossing method using a Carver Laboratory Press (Model M Carver Inc., Wabash, IN). An imprint template for hot embossing was fabricated as described elsewhere.<sup>40</sup> An ATR-FTIR spectrometer (Vertex 70, Bruker Corp.) was interfaced with the MF device using a single reflection diamond ATR crystal (MIRacle, Pike Technologies). The fluidic connections were interfaced with the MF device using an interface component (FlowJEM Inc.). A detailed description of the fabrication of the MF device and an integration of the ATR crystal are provided in Supporting Information.

Multilayer films of polyacrylic acid and polyallylamine hydrochloride (LbL films) were prepared using a static dipping method.<sup>37</sup> The dip-wash-dip process was repeated for 5 times. The same LbL films were prepared under flow conditions on the surface of silicon wafer that was covered by a microchannel.<sup>35</sup> The details of film preparation are given in Supporting Information. The thickness of the dried LbL film was measured using Dektak XT surface profilometer.

## Experimental design

A MF device comprising a microchannel with a width and height of 200 and 50 µm, respectively, was fabricated in polycarbonate (see Supporting Information). The device was integrated with a diamond ATR crystal with a diameter of 1.8 mm (Fig. 1a, b and c), as described elsewhere.<sup>32</sup> A microscopy image of the channel segment integrated with the ATR crystal is shown in Fig 1b. The

polymer solution was supplied to the MF device using a syringe pump (PHD 2000, Harvard Apparatus) at a constant volumetric flow rate,  $Q$ . After a particular time, typically, 25 min, the supply of the polymer solution was terminated and deionized water was introduced into the channel to remove the free and loosely-adsorbed polymer from the system. Fig. 1d-f illustrates different stages of the experimental study of polymer adsorption in flow: (i) exposure of the ATR crystal surface (a substrate) to an aqueous polymer solution introduced in the MF device; (ii) polymer adsorption onto the crystal surface, reaching a steady state after a particular time interval; and (iii) the removal of the loosely surface-attached and free polymer by insertion of deionized water at a volumetric flow rate  $Q_w$ .

The IR spectra were collected in the course of polymer adsorption and after the washing step. The spectra were generated from 32 scans at 10 kHz with 4 cm<sup>-1</sup> spectral resolution. The computer-controlled data acquisition and analysis of the spectra were performed using Opus 6.5 software.

To form a multilayer LbL polymer film on the surface of the ATR crystal, alternating streams of PAA and PAH solutions were introduced in the MF device, with the washing step between the infusion of each polymer solution. The IR spectra were acquired after each washing step.

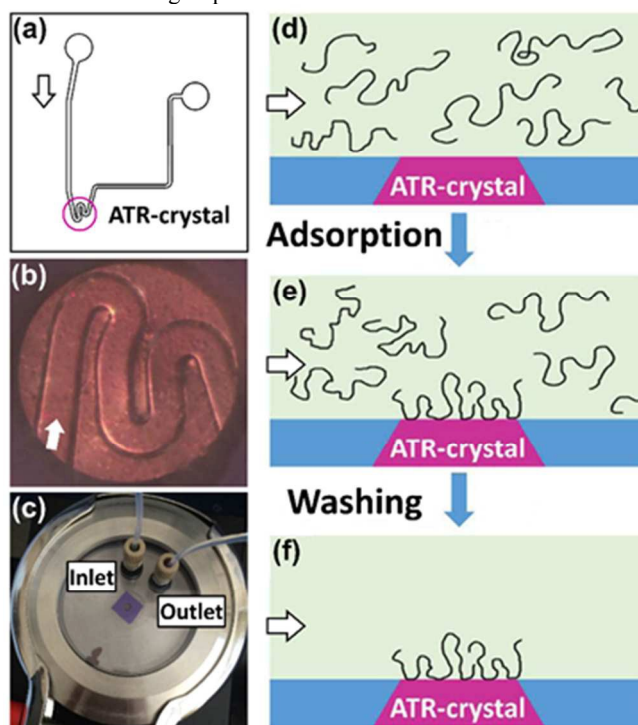


**Fig. 1** Polymer adsorption on the surface of ATR crystal integrated with the MF device. (a) Design of the MF channel. The arrow indicates the direction of flow of the polymer solution. The red circle shows the position of the ATR crystal. (b) Optical microscopy image (top view) of the fragment of the microchannel interfaced with a circular ATR crystal. (c) Photograph of the MF device integrated with an ATR crystal. (d-f) Three stages of studies of polymer adsorption: infusion of the polymer solution with a particular concentration in the MF device (d); polymer adsorption on the ATR crystal surface (e); washing of the loosely-attached and non-adsorbed polymer with deionized water (f), leaving strongly adsorbed polymer on the crystal surface. The horizontal arrows in (d-f) indicate the direction of flow of the polymer solution.

## Results and discussion

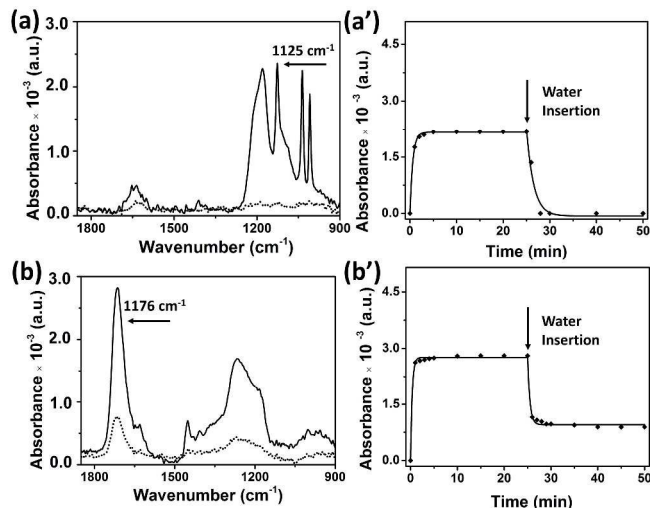
To explore the feasibility of MF studies of polymer adsorption in flow, we used two exemplary anionic polyelectrolytes, namely, polystyrene sulfonate (PSS) and polyacrylic acid (PAA). Fig. 2a shows the IR spectra of PSS after 25 min-long introduction of the polymer solution in the MF device (solid line) and 25 min-long injection of deionized water (dashed line). Two characteristic peaks at 1178  $\text{cm}^{-1}$  and 1125  $\text{cm}^{-1}$  correspond to the asymmetric stretching vibrations of the S=O; the bending at 1037  $\text{cm}^{-1}$  was assigned to the S=O symmetrical stretching vibrations, and the peak at 1008  $\text{cm}^{-1}$  was attributed to aromatic in-plane vibrations.<sup>42</sup> Adsorption of PSS on the ATR crystal surface was characterized by monitoring the intensity of the peak at 1125  $\text{cm}^{-1}$  (indicated with an arrow in Fig. 2a). The IR spectra of PAA before and after washing steps are shown in Fig. 2b. A sharp narrow peak at 1726  $\text{cm}^{-1}$ , indicated by an arrow, corresponds to C=O stretching, and a weaker, broader peak at 1285  $\text{cm}^{-1}$  corresponds to the C-O stretching.<sup>42</sup> The time-dependent intensity of the peak at 1726  $\text{cm}^{-1}$  was monitored to study PAA adsorption.

Fig 2a' and b' shows the variation in intensity of the characteristic absorbance peaks of PSS and PAA, respectively, as a function of the time of flow of the corresponding polymer solutions past the ATR crystal. For PSS, the value of absorbance intensity increased with infusion time and in 4 min after the polymer solution reached the crystal surface, the intensity reached a steady state (Fig 2a'). Following infusion of deionized water for 5 min, the IR signal reduced to zero, indicating that free and weakly adsorbed PSS were completely removed from the system.

In contrast, adsorption of PAA exhibited different features. First, similar to PSS, after initial increase in absorbance intensity, 6 min after the solution reached the ATR crystal surface, the intensity of C=O stretching peak reached a constant value. After injection of deionized water for 5 min, absorbance intensity reduced by ~60 % and leveled off (25 min-long injection of water did not cause any further changes in absorbance intensity). Thus, we conclude that in contrast to PSS, after the washing step, PAA remained adsorbed to the surface of the ATR-crystal.

The difference in adsorption of PSS and PAA was rationalized as follows. At pH=7.0, PSS exists in the solution in a salt form. Due to the full dissociation and ionization of the  $-\text{SO}_3\text{H}$  group ( $\text{pK}_a$  of  $-\text{SO}_3\text{H}$  is 1.85),<sup>43</sup> PSS molecules have a lower propensity to adsorb to the ATR-crystal surface. In control experiments conducted for PSS solutions at pH=2 from 1.0 M NaCl solution, PSS strongly adsorbed onto the crystal surface (see Supporting Information). On the other hand, PAA is a weak acid with  $\text{pK}_a=4.25$ .<sup>43</sup> At pH=3.5, PAA molecules were in a non-ionized state and due to the poor solvency condition had a higher propensity to adsorb to the ATR-crystal surface. Further studies of polymer adsorption in flow described in the present work have been conducted for PAA.

First, we examined the effect of the flow rate of the solution of PAA on polymer adsorption. A PAA solution at polymer concentration  $C_{\text{PAA}}=5$  mg/mL was supplied for 25 min to the MF device at a flow rate varying from 0.5 to 15.0 mL/hr (corresponding to the linear velocity from 0.35 to 10.5 mm/s or the shear rate from 7 to 210  $\text{s}^{-1}$ ). For solution viscosity in the range from 30 cP (at the shear rate of 210  $\text{s}^{-1}$ ) to 43 cP (at the shear rate of 7  $\text{s}^{-1}$ ), the calculated shear stress applied was from 300 to 6300 Pa. Subsequently to that, the ATR crystal surface was washed with deionized water for 25 min. Fig. 3a shows that the variation in flow rate of the PAA solution had little effect on absorbance intensity and hence, on the amount of polymer adsorbed on the ATR crystal.

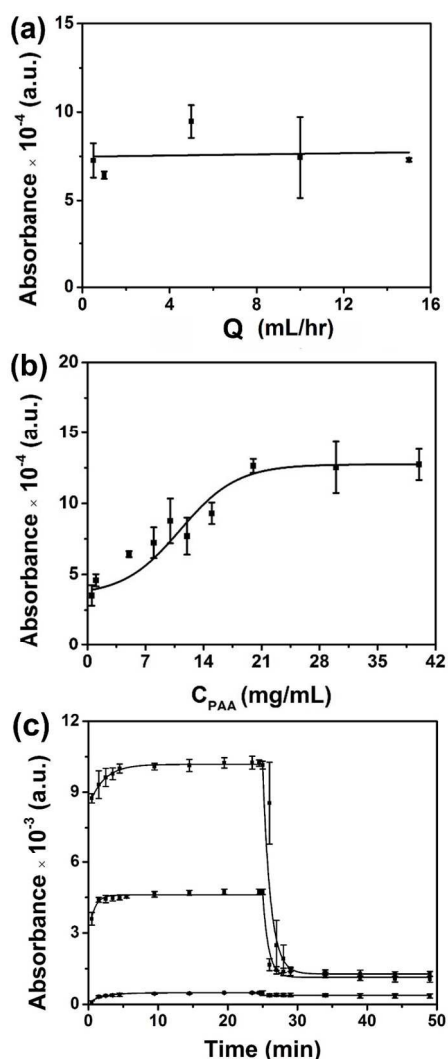


**Fig. 2** Characterization of adsorption of PSS and PAA. IR absorption spectra of PSS (a) and PAA (b), both acquired after 25 min-long infusion of the polymer solution (solid lines) and after 25 min-long washing step (dotted lines). Polymer concentration in both solutions was 8 mg/mL. The arrows show the IR peaks used for the characterization of polymer adsorption. The flow rate of the polymer solutions and deionized water in the washing step was 1 mL/hr.

In the next series of experiments, the effect of the concentration, of the PAA solution was examined for  $0.5 \leq C_{\text{PAA}} \leq 40$  mg/mL. As shown in Fig. 3b, for  $C_{\text{PAA}} \leq 20$  mg/mL, the absorbance intensity of C=O group increased with polymer concentration, indicating that a larger amount of PAA adsorbed to the surface. At  $C_{\text{PAA}} > 20$  mg/mL, absorbance leveled off, suggesting that a saturated polymer layer formed on the surface.

Fig 3c shows the variation in intensity of the characteristic PAA absorption peak, plotted as a function of time of insertion of the PAA solution in the MF device and the time of washing. The experiments were conducted for three values of  $C_{\text{PAA}}$  of 0.5, 15 and 40 mg/mL at  $Q=1$  mL/hr. For all solutions, a steady state absorbance was reached in ~5 min after the polymer solution front reached the ATR crystal surface. When  $C_{\text{PAA}}$  increased from 0.5 to 15 mg/mL, the amount of adsorbed PAA notably increased after washing, however, no significant change in adsorption occurred upon further increase in  $C_{\text{PAA}}$  from 15 to 40 mg/mL. The latter effect suggested the formation of the saturated PAA layer at  $C_{\text{PAA}}=15$  mg/mL.

Next, we explored the effect of pH of the solution on PAA adsorption. Phosphate, Tris, and Piperidine buffers were used to adjust the value of pH of PAA solutions to 2, 8 and 11, respectively. For the PAA solution at pH 8 and 11, Fig. 4 b, c and d show the characteristic symmetric and asymmetric stretching bends of the  $\text{COO}^-$  group at 1408 and 1562  $\text{cm}^{-1}$ , respectively, and the  $\text{CH}_2$  stretching frequency at 1453  $\text{cm}^{-1}$ .<sup>42</sup> For pH=2 (Fig. 4e and f), the IR spectra exhibited the stretching bend of C=O group at 1717  $\text{cm}^{-1}$ , the  $\text{CH}_2$  stretching bend at 1455  $\text{cm}^{-1}$ , and the C-O stretching bend at 1265  $\text{cm}^{-1}$ .<sup>42</sup> The characteristic peaks used to analyze the adsorption behavior of PAA are specified by arrows in Fig. 4. We also examined the effect of ionic strength on PAA adsorption by adding an electrolyte NaCl to the polymer solution to the concentration  $C_{\text{NaCl}}$  of 0.1 and 1 M.



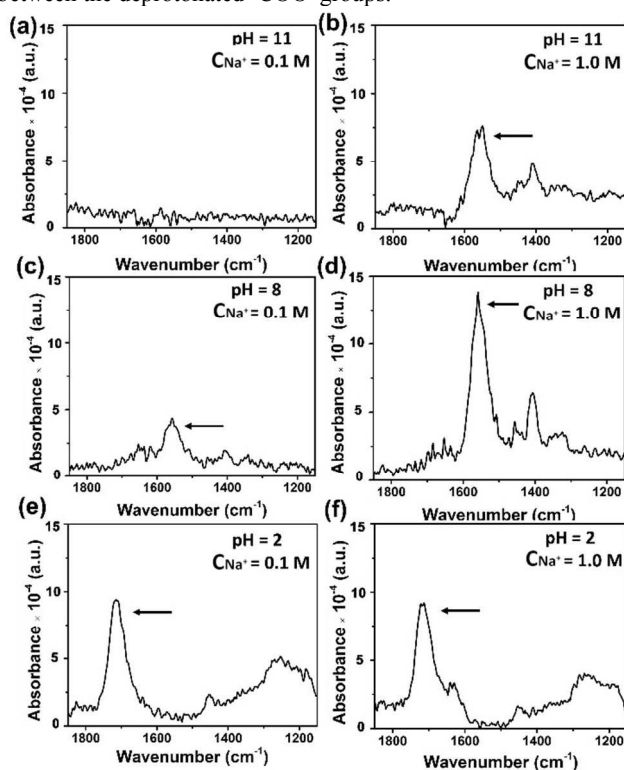
**Fig. 3** Variation in absorbance, plotted as a function of velocity of PAA solution (a) and PAA concentration,  $C_{PAA}$ , in the solution (b). In (a)  $C_{PAA} = 5$  mg/mL. In (b)  $Q = 1$  mL/hr. All experiments included 25 min infusion PAA solution and 25 min-long washing step. (c) Temporal variation in absorbance  $C_{PAA}$  (bottom to top) of 0.5, 15 and 40 mg/mL, all monitored over polymer infusion time and washing time. In (a-c), each experimental point represents the average of the results of three independent experiments.

Fig. 4a shows that at  $pH = 11$  and  $C_{NaCl} = 0.1$  M, the PAA did not adsorb to the surface, however upon an increase in the ionic strength (Fig. 4b), a decrease in pH (Fig. 4c), or at a simultaneous change in both characteristics (Fig. 4d), polymer adsorption took place. An increase of an ionic strength of the solution did not affect the spectral position of the characteristic IR band of PAA, but resulted in a stronger adsorption of PAA (compare Fig. 4a and b or Fig. 4c and d). When the COOH group of PAA was not ionized at  $pH = 2$ , an increase in ionic strength of the solution had little effect on polymer adsorption (Fig. 4e and f). The PAA adsorption on the ATR crystal surface decreased with an increasing pH of the solution, as evidenced by comparing Fig. 4a and c (or 4b and d) at the same NaCl concentration.

These results agree with the existing mechanism of polyelectrolyte adsorption, in which the ionization state of charged groups largely determines the quality of the solvent for the

polymer.<sup>45,46</sup> At high pH values and low ionic strength, the quality of the solvent for PAA was improved, which counteracted its adsorption on the ATR crystal surface. For  $pH < pK_a$ , the protonated  $-COOH$  groups are the most prevalent, and PAA readily adsorbed on the crystal from a poor solvent.

In principle, the IR spectra of the adsorbed polymer could provide information on the change in PAA conformation with pH, since at  $pH > pK_a$ , PAA molecules undergo a transition from the globular state to the rod-like configuration,<sup>46</sup> which is most likely preserved on the surface.<sup>4</sup> Yet, at  $pH = 2$  (below  $pK_a$ ) and pH of 8 and 11 (above  $pK_a$ ), different characteristic bands were monitored, thereby precluding comparison of the spectral position of the IR peaks. We note however a small difference in the position of the asymmetric stretching bend of the  $COO^-$  group from 1560 to 1553  $cm^{-1}$ , when pH increased from 8 to 11, respectively, in 1M NaCl solution. This shift may reflect the change in the stretched configuration of PAA molecules, due to electrostatic repulsion between the deprotonated  $-COO^-$  groups.<sup>47</sup>



**Fig. 4** IR adsorption spectra of PAA solution after washing under different pH values and ionic strengths. The solution pH was set to 11 (a, b), 8 (c, d), and 2 (e, f). The ionic strength was tuned by controlling the concentration of NaCl in the polymer solutions to 0.1 M (a, c, e), or 1.0 M, (b, d, f). The time for infusing and washing are both 25 min. The flow rate was kept at 1 mL/hr.

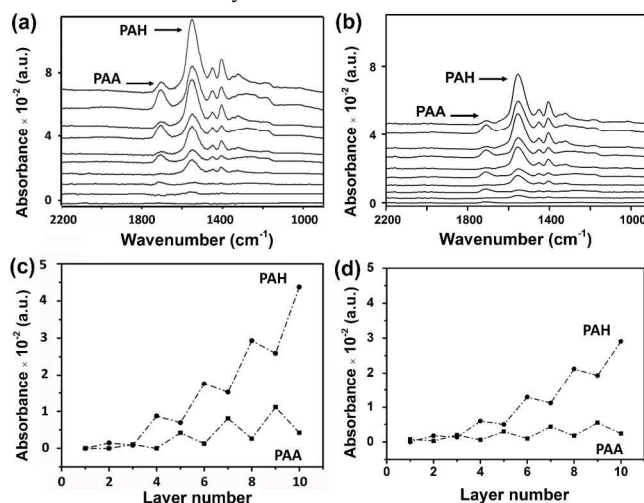
Finally, we utilized the MF-IR method to monitor in-flow layer-by-layer (LbL) adsorption of alternating polymer layers formed by the anionic PAA and cationic PAH molecules. Following 5 min injection of the PAA solution ( $C_{PAA} = 2$  mg/mL,  $Q = 1$  mL/hr) and a subsequent washing step with a deionized water, we introduced in the MF device a solution of PAH at the same concentration, flow rate, and insertion time as those of PAA solution. These two steps were repeated 5 times and the IR spectra were collected after each washing step.

Fig. 5a shows the corresponding IR spectra of PAA and PAH,

which exhibit the N-H stretching band at  $1560\text{ cm}^{-1}$ , characteristic for PAH, and the C=O stretching band of COOH group at  $1726\text{ cm}^{-1}$ , characteristic for PAA. Thus we monitored changes in IR spectra in the  $1400\text{--}1800\text{ cm}^{-1}$  spectral region, to study adsorption of PAA and PAH.

Absorbance intensity of the peak at  $1726\text{ cm}^{-1}$  increased after the injection of the PAA solution and decreased after the infusion of the solution of PAH. Similarly, absorbance intensity of the peak at  $1560\text{ cm}^{-1}$  increased with addition of PAH in the system and decreased with addition of PAA (Fig. 5a). The variation in absorbance intensity of the characteristic peaks of PAA and PAH, both after the washing steps, is plotted in Fig. 5c as a function of the layer number (odd number for infusion of PAA and even number for infusion of PAH). Adsorption of both polymers exhibited a step-wise profile. The change in intensity of the peak  $1560\text{ cm}^{-1}$  was notably stronger than at  $1726\text{ cm}^{-1}$ , due to the additional contribution of COO<sup>-</sup> group of PAA, due to deprotonation of the COOH group after infusion of PAH (pH=7.0).<sup>48</sup> Thus with every addition of PAH, the intensity of the COOH band was reduced, whereas the peak at  $1560\text{ cm}^{-1}$  was increased. Upon the addition of PAA solution (pH=3.5) these groups were protonated, again. Another reason for the stronger change in PAH absorption, leading to the asymmetric growth of two polyelectrolyte multilayers, could originate from charge overcompensation at the surface, which occurred mostly upon the addition of a polycation.<sup>46</sup>

In addition, we conducted IR characterization of PAA and PAH layers adsorbed under quiescent conditions. The corresponding IR spectra of PAA and PAH are shown in Fig. 5b and the variations in absorbance intensity of the characteristic peaks of PAA and PAH, both after the washing steps, are plotted in Fig. 5d. Compared with the quiescent conditions, the IR spectra of both PAA and PAH adsorbed in flow exhibited characteristic bands with higher intensities. This effect indicated that flow favoured LbL adsorption, presumably to the shear-induced exposure of functional groups responsible for adsorption in the preceding polymer layer adsorbed to the ATR crystal.



**Fig. 5.** Infrared spectra of alternating PAA and PAH layers adsorbed under flow (a) and quiescent (b) conditions. The concentration of PAA and PAH solutions was  $2\text{ mg/mL}$ . The values of pH were 3.5 and 7.0 for solutions of PAA and PAH, respectively. In MF experiments, the time of solution infusion was 5 min, which was followed by a 5 min washing with deionized

water. The flow rate of the polymer solutions and deionized water was  $1\text{ mL/hr}$ . For the quiescent adsorption experiments, the solution was introduced onto the ATR-crystal and incubated for 5 min before washing with deionized water. (c, d) Variation in intensity of  $1726\text{ cm}^{-1}$  (corresponding to PAA) and  $1560\text{ cm}^{-1}$  (corresponding to PAH) peaks, following the formation of each successive layer under flow (c) and static (d) conditions. Odd numbers of layers represent those with the outmost PAH layer; even numbers of layers represents those with the PAA outmost layer.

To validate a MF-IR methodology, we examined the thickness of alternating PAA and PAH layers formed by adsorption in-flow (shear rate  $69.4\text{ s}^{-1}$ ) and under static conditions by using surface profilometry. Adsorption in flow was carried out under conditions similar to MF-IR experiments. Fig. 6 shows that under in-flow conditions, the build-up of the polymer layers was faster than that under the static conditions. Furthermore, in contrast to static conditions, polymer layer growth occurred in a non-linear manner, in agreement with IR-MF experiments (Fig. 5). In particular, in static conditions, the average thickness of the PAA/PAH bilayer was  $12\text{ nm}$ , in agreement with earlier reported results,<sup>45</sup> while the average thickness of the PAA/PAH bilayers formed in flow was  $17.1\text{ nm}$ . A larger thickness of the polymer bilayer adsorbed under flow could be presumably caused by the change in polymer conformation (a larger number of loops), due to the shear stress imposed on the polymer chains during adsorption process.<sup>44</sup>

The results shown in Fig. 5 have at least, two important implications. First, they show that the MF-IR platform can be used to monitor adsorption of multicomponent polymer layers with distinct IR signatures. Second, these results demonstrate the capability of modification of the surface with an appropriate "primer" layer, which strongly and selectively interacts with the polymer of interest. Finally, based on Figs. 5 and 6, LbL adsorption in flow differs from multilayer adsorption under quiescent conditions. The detailed investigation of this effect needs further investigation.

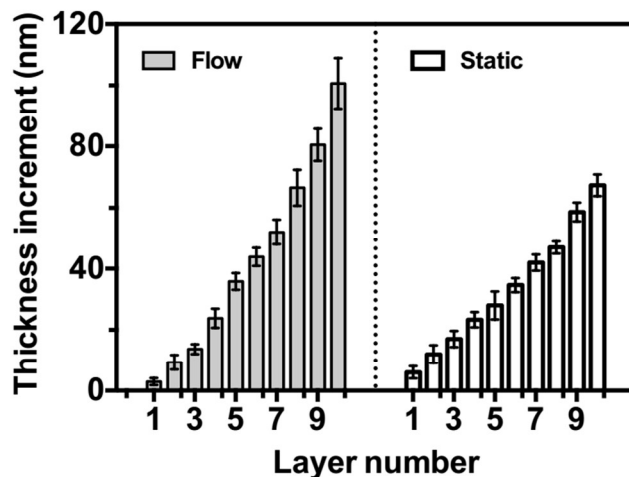


**Fig. 6** Variation in thickness of PAA/PAH LbL film adsorbed under flow (left) and static (right) conditions. Each bilayer was prepared using PAA solution at pH=3.5 and PAH solution at pH=7.0 at the incubation time of 5 min. The film was rinsed with deionized water and air-dried before the measurement. Odd numbers of layers represent those with the outmost PAA layer and even numbers of layers represents the film with the PAH outmost layer. The

concentration of PAA and PAH solutions ( $C_{\text{PAA}}$  and  $C_{\text{PAH}}$ ) are 2 mg/mL. Injection flow rates of PAA solution, water and PAH solution were 1.0 mL/hr. Under both conditions, each experimental point represents the average of the results of three independent experiments.

## Conclusions

A MF-IR platform was developed for in-situ studies of polymer adsorption from solutions flowing past a solid surface. Adsorption of polyelectrolytes was studied under varying flow rates, polymer concentrations, pH, and ionic strengths of the solution. The platform was also used to study layer-by-layer adsorption of polyacrylic acid and polyallylamine hydrochloride. Comparison of LbL adsorption in flow and under quiescent conditions showed a stronger polymer adsorption in the former case, the effect that needs further investigation. The developed methodology paves the way for studies of in-flow adsorption of biomacromolecules and their supramolecular assemblies, including proteins, nucleic acids and polysaccharides, thereby mimicking important biological processes occurring *in vivo*.

## Acknowledgements

ZW, DV and EK thank NSERC Canada (Discovery grant) for financial support of this work. DV acknowledges Microfluidic Applications and Training in Cardiovascular Health (MATCH) Scholarship. WL thanks New Faculty Startup Funds from Texas Tech University

## Notes and references

<sup>a</sup> Department of Chemistry, University of Toronto, 80 Saint George street, Toronto, Ontario, Canada M5S 3H6. E-mail: ekumache@chem.utoronto.ca; Fax: +1 416-978-3576; Tel: +1 416-978-3576

<sup>b</sup> State Key Laboratory of Supramolecular Structure and Materials, Department of Chemistry, Jilin University, Changchun, Jilin, China 130012; E-mail: wangzhaoyi1988@gmail.com

<sup>c</sup> Department of Oncology, Tongji Hospital, Tongji Medical College, Huazhong University of Science and Technology, Wuhan, China, 430030; E-mail: ltang@tjh.tjmu.edu.cn

<sup>d</sup> Department of Chemical Engineering, Texas Tech University, Lubbock, Texas, 79409-3121, United States America; E-mail: wei.li@ttu.edu; Tel: +1 806-834-2209

† Electronic Supplementary Information (ESI) available: [details of any supplementary information available should be included here]. See DOI: 10.1039/b000000x/

## References

- T. Ramanathan, A. A. Abdala, S. Stankovich, D. A. Dikin, M. Herrera-Alonso, R. D. Piner, D. H. Adamson, H. C. Schniepp, X. Chen, R. S. Ruoff, S. T. Nguyen, I. A. Aksay, R. K. Prud'homme and L. C. Brinson, *Nat. Nanotechnol.*, 2008, **3**, 327-331.
- H. Zheng, *Polymer Adsorption, Friction, and Lubrication*, Hoboken, New Jersey: Wiley, 2013.
- D. F. Evans, H. Wennerström, *The Colloidal Domain: Where Physics, Chemistry, Biology and Technology Meet*, 2nd ed., Wiley-VCH: New York, 1999.
- G. J. Fleer, M. A. Cohen Stuart, J. H. M. H. Scheutjens, T. Cosgrove, B. Vincent, *Polymers at Interfaces*, Chapman & Hall: London, 1993.
- S. Granick, S. K. Kumar, E. J. Amis, M. Antonietti, A. C. Balazs, A. K. Chakraborty, G. S. Grest, C. Hawker, P. Janmey, E. J. Kramer, R. Nuzzo, T. P. Russell and C. R. Safinya, *J. Polym. Sci. Part B: Polym. Phys.*, 2003, **41**, 2755-2793.
- Handbook of Environmental Engineering, V. 13: Membrane and Desalination Technologies, L.K. Wang et al., Eds. Chapter 7, 312-315. Compans, Richard W. Cooper, Max D. Honjo, Tasuku, Bacterial Biofilms, Springer, 2008
- K. B. Neeves, A. A. Onasoga and A. R. Wufsus, *Curr. Opin. Hematol.*, 2013, **20**, 417-423.
- J. Lee and G. G. Fuller, *Macromolecules*, 1984, **17**, 375-380.
- V. Shubin and P. Linse, *J. Phys. Chem.*, 1995, **99**, 1285-1291.
- S. Schwarz, K.-J. Eichhorn, E. Wischerhoff and A. Laschewsky, *Colloids Surf. A*, 1999, **159**, 491-501.
- A. R. Al-Hashmi and P. F. Luckham, *Colloids and Surfaces A: Physicochem. Eng. Aspects*, 2012, **393**, 66-72.
- R. W. Watkins and C. R. Robertson, *J. Biomed. Mater. Res.*, 1977, **11**, 915-938.
- M. A. Bos and J. M. Kleijn, *Biophys. J.*, 1995, **68**, 2566-2572.
- M. A. Bos and J. M. Kleijn, *Biophys. J.*, 1995, **68**, 2573-2579.
- E. Pefferkorn, A. Carroy and R. Varoqui, *J. Polym. Sci. B Pol. Phys.*, 1985, **23**, 1997-2008.
- F. Caruso, T. Serizawa, D. N. Furlong and Y. Okahata, *Langmuir*, 1995, **11**, 1546-1552.
- P. Frantz, D. Perry and S. Granick, *Colloids and Surfaces A: Physicochem. Eng. Aspects*, 1994, **86**, 295-298.
- F. Zaera, *Chem. Rev.*, 2012, **112**, 2920-2986.
- S. Iwao and S. Granick, *Langmuir*, 1998, **14**, 4266-4271.
- H. E. Johnson and S. Granick, *Macromolecules*, 1990, **23**, 3367-3374.
- M. J. Baker, J. Trevisan, P. Bassan, R. Bhargava, H. J. Butler, K. M. Dorling, P. R. Fielden, S. W. Fogarty, N. J. Fullwood, K. A. Heys, C. Hughes, P. Lasch, P. L. Martin-Hirsch, B. Obinaju, G. D. Sockalingum, J. Sulé-Suso, R. J. Strong, M. J. Walsh, B. R. Wood, P. Gardner and F. L. Martin, *Nat. Protoc.*, 2014, **9**, 1771-1791.
- G. M. Whitesides, *Nature*, 2006, **442**, 368-373.
- K. R. Hawkins, M. R. Steedman, R. R. Baldwin, E. Fu, S. Ghosal, and P. Yager, *Lab Chip*, 2007, **7**, 281-285.
- E. Karabudak, B. L. Mojet, S. Schlautmann, G. Mul and H. J. G. E. Gardeniers, *Anal. Chem.*, 2012, **84**, 3132-3137.
- M. Müller, T. Rieser, K. Lunckwitz, S. Berwald, J. Meier-Haack, D. Jehnichen, *Macromol. Rapid Commun.*, 1998, **19**, 333-336.
- J. Greener, B. Abbasi and E. Kumacheva, *Lab Chip*, 2010, **10**, 1561-1566.
- D. Voicu, C. Scholl, W. Li, D. Jagadeesan, I. Nasimova, J. Greener and E. Kumacheva, *Macromolecules*, 2012, **45**, 4469-4475.
- K. L. A. Chan and S. G. Kazarian, *Anal. Chem.*, 2012, **84**, 4052-4056.
- S.G. Kazarian and K.L.A. Chan, *Biochimica et Biophysica Acta*, 2006, 1758, 858-867.
- K. L. A. Chan, S. Gulati, J. B. Edel, A. J. de Mello and S. G. Kazarian, *Lab Chip*, 2009, **9**, 2909-2913.
- J. Greener, W. Li, J. Ren, D. Voicu, V. Pakhareenko, T. Tang and E. Kumacheva, *Lab Chip*, 2010, **10**, 522-524.
- G. Decher, *Science*, 1997, **277**, 1232-1237.
- A. Finnemore, P. Cunha, T. Shean, S. Vignolini, S. Guldin, M. Oyen and U. Steiner, *Nat. Commun.*, 2012, **3**, 966-972.
- S. A. Castleberry, W. Li, D. Deng, S. Mayner and P. T. Hammond, *ACS Nano*, 2014, **8**, 6580-6589.
- P. Lavalle, J. C. Voegel, D. Vautier, B. Senger, P. Schaaf and V. Ball, *Adv. Mater.*, 2011, **23**, 1191-1221.
- D. Yoo, S. S. Shiratori and M. F. Rubner, *Macromolecules*, 1998, **31**, 4309-4318.
- A. Fery, B. Schöler, T. Cassagneau and F. Caruso, *Langmuir*, 2001, **17**, 3779-3783.
- W. C. Chan, D. T. Elmore, E. Farkas, A. Higton, B. Penke, I. Sovago, G. Toth and G. Varadi, *Amino Acids, Peptides and Proteins*, The Royal Society of Chemistry, Cambridge, UK, 2006.
- G. Decher and J. Schlenoff, *Multilayer thin films: sequential assembly of nanocomposite materials*, Wiley-VCH, Weinheim, Germany, 2003.
- M. Müller, ATR-FTIR spectroscopy at polyelectrolyte multilayer systems. In *Handbook of Polyelectrolytes and Their Applications*; Tripathy, S.K., Kumar, J., Nalwa, H.S., Eds.; American Scientific Publishers (ASP): Valencia, CA, USA, 2002; Volume 1, pp. 293-312.
- K. G. R. Pachler, F. Matlok, H. U. Gremlich, Merck FT-IR atlas: a collection of FT-IR spectra, VCH: Weinheim, New York, 1988.
- D. R. Lide, ed., *CRC Handbook of Chemistry and Physics*, Internet Version, 2005.

- 
- 44 L. J. Kirwan, P. D. Fawell and W. van Bronswijk, *Langmuir*, 2003, **19**, 5802-5807.
- 45 S. S. Shiratori and M. F. Rubner, *Macromolecules*, 2000, **33**, 4213-4219.
- 5 46 R. A. Ghostine, M. Z. Markarian and J. B. Schlenoff, *J. Am. Chem. Soc.*, 2013, **135**, 7636-7646.
- 47 D. A. Beattie, J. Addai-Mensah, A. Beaussart, G. V. Franks and K. Yeap, *Phys. Chem. Chem. Phys.*, 2014, **16**, 25143-25151.
- 48 J. D. Mendelsohn, C. J. Barrett, V. V. Chan, A. J. Pal, A. M. Mayes  
10 and M. F. Rubner, *Langmuir*, 2000, **16**, 5017-5023.